

## A SCALING RELATION BETWEEN MERGER RATE OF GALAXIES AND THEIR CLOSE PAIR COUNT

C. Y. JIANG<sup>1</sup>, Y. P. JING<sup>2</sup>, JIAXIN HAN<sup>3</sup>,

## ABSTRACT

When the galaxy merger rate is measured from the observed close pair count, usually a single merger timescale is assumed. Current calibrations based on simulations have focused mostly on major mergers (stellar mass ratios from 1:1 to 1:4). Using a high-resolution N-body/SPH cosmological simulation, we find an accurate scaling relation between galaxy pair counts and merger rates down to a stellar mass ratio of about 1:30. The relation explicitly accounts for the dependence on redshift (or time), pair separation, and virial masses of the two galaxies in a pair. With this relation, one can easily obtain the mean merger timescale for a close pair of galaxies. The use of virial masses, instead of the stellar mass, is motivated by the fact that the dynamical friction time scale is mainly determined by the dark matter surrounding central and satellite galaxies. This fact can also minimize the error induced by uncertainties in modeling star formation in the simulations. Since the virial mass can be read from the well-established relation between the virial masses and the stellar masses in observation, our scaling relation can be easily applied to observations to obtain the merger rate and merger time scale. For major merger pairs (1:1-1:4) of galaxies above  $4 \times 10^{10} h^{-1} M_{\odot}$  at  $z = 0.1$ , it takes about 0.31 Gyr to merge for pairs within a projected distance of  $20 h^{-1} \text{kpc}$  with stellar mass ratio of 1:1, while the time taken goes up to 1.6 Gyr for mergers with stellar mass ratio of 1:4. Our results indicate that a single timescale is not enough to describe mergers with the stellar mass ratio spanning even a narrow range from 1:1 to 1:4.

*Subject headings:* dark matter — galaxies: clusters: general — galaxies: kinematics and dynamics — methods: numerical

## 1. INTRODUCTION

Estimating merger rates and merger timescales of galaxies is crucial to studies of galaxy growth. Especially for early-type galaxies, merger rates are decisive in quantifying their mass assembly history and size increase process. It determines whether the frequency of mergers is appropriate for the observed mass/size growth of the early-type galaxies (Nipoti et al. 2009, 2012; Chou et al. 2011; Cimatti et al. 2012; Newman et al. 2012; McLure et al. 2013).

In observational studies, merger rates are usually converted from the number of close pairs. The authors generally assume that galaxies within some projected distance (e.g.,  $20 h^{-1} \text{kpc}$ ) would merge in a constant timescale (around 0.5 Gyr) after accounting for the projection effects (Patton et al. 2000, 2002; Bell et al. 2006; De Propris et al. 2007; Lin et al. 2004, 2008; Patton & Atfield 2008). Kitzbichler & White (2008) checked these assumptions using semi-analytic catalogues derived from the Millennium Simulation (Springel 2005). They found that the merger timescales in their results are typically larger by a factor of 2 than the constant timescale that is usually assumed. In their semi-analytical model, they traced the dynamics of satellite galaxies through following the subhalos these galaxies reside in. Once the surrounding subhalo is tidally dis-

rupted, the galaxy is assumed to merge with its central galaxy after a dynamical friction time. It is parametrized as in Binney & Tremaine (1987), but multiplied by a fudge factor 2 (De Lucia & Helmi 2008), to account for the underestimation of the dynamical friction times in Binney & Tremaine (1987). The timescales on which close galaxies within a certain distance would merge, are therefore dependent on the dynamical times they adopted. However, Jiang et al. (2008) showed that the theoretical dynamical friction times are underestimated by a factor depending on both the mass ratio and the satellite's orbit. On the other hand, Kitzbichler & White (2008) only considered major mergers with stellar mass ratios larger than 1:4. It is hence restricted to major merger studies, but not applicable for investigating galaxy growth through minor mergers, which are currently considered the most promising mechanism for the size evolution of early compact massive galaxies (Bezanson et al. 2009; Naab et al. 2009; Hilz et al. 2012; Oogi & Habe 2013).

Lotz et al. (2008, 2010a,b, 2011) analysed the timescales for mergers identified both with quantitative morphology and with close pairs using N-body/SPH simulations. For close pair timescales, they first studied individual merger pairs for several different projected separation criteria, seeking the dependence on mass ratio, gas fraction and orbits. To obtain the cosmologically-averaged merger timescale, they extracted the distributions of baryonic mass ratio and gas fraction from three cosmological-scale galaxy evolution models. Then they computed the average merger timescale by weighting the individual timescale with these distributions. They found that the timescale depends mainly on the outmost radius adopted to identify close pairs for major (1:1-1:4) mergers. However,

<sup>1</sup> Key Laboratory for Research in Galaxies and Cosmology of Chinese Academy of Sciences, Shanghai Astronomical Observatory, Nandan Road 80, Shanghai 200030, China

<sup>2</sup> Center for Astronomy and Astrophysics, Department of Physics and Astronomy, Shanghai Jiao Tong University, Shanghai 200240, China; [ypjing@sjtu.edu.cn](mailto:ypjing@sjtu.edu.cn)

<sup>3</sup> Institute for Computational Cosmology, Department of Physics, University of Durham, Science Laboratories, South Road, Durham DH1 3LE, UK

they did not consider the case of minor mergers for close pairs either. Later, [Xu et al. \(2012\)](#) combined the results in [Lotz et al. \(2010a\)](#) with the mass dependence and redshift dependence in [Kitzbichler & White \(2008\)](#), giving a description for timescales of major mergers with projected distance between  $5 h^{-1}\text{kpc}$  and  $20 h^{-1}\text{kpc}$ .

In this work, we study the relation between the galaxy merger rate and number of close pairs using a cosmological N-body/SPH simulation. We give an empirical calibration of this relation by taking into account diverse factors, including the redshift, pair separation, and the virial masses that the two galaxies in a pair correspond to, respectively.

## 2. METHODS

We use an N-body/SPH simulation run with Gadget2 code ([Springel 2005](#)) to calibrate the relation between galaxy merger rates and close pair counts. For the detailed description of the simulation and the post-processing, the readers are referred to [Jiang et al. \(2008\)](#). By default, galaxies are identified with the friends-of-friends method, in which a linking-length of 0.025 times the mean inter-particle separation is applied to stellar particles.

As usual, two galaxy samples are defined in searching for close pairs. Galaxies in the primary sample are targeted to count their close neighbors from the secondary sample.

The volume merger rate can be written as

$$\Phi = C_{\text{mg}} n_1 n_p(< r_p) / T_{\text{mg}}, \quad (1)$$

where  $n_1$  is the number density of the primary sample, and  $n_p(< r_p)$  is the number of close companions within a distance of  $r_p$  for each galaxy in the primary sample.  $T_{\text{mg}}$  is the typical timescale for galaxies at  $r_p$  to merge. The coefficient  $C_{\text{mg}}$  describes the fraction of pairs that are bound to merge in a typical timescale  $T_{\text{mg}}$ . Here the primary sample and the secondary sample are exclusive to each other.

The major mechanism that drives the merging of the two galaxies in close companion is dynamical friction, which would exhaust the orbital energy of the satellite after a certain timescale. Therefore, we tentatively formulate the merging timescale  $T_{\text{mg}}$  in the form of dynamical friction timescale,  $T_{\text{mg}} \propto \frac{v_c r_p^2}{G m_2 \ln \Lambda}$  ([Binney & Tremaine 1987](#)), where  $v_c$  is the circular velocity of the primary halo assuming an isothermal sphere, and  $m_2$  is the satellite mass. Although the galaxy pairs are close in distance, some may have higher orbital energy that is equivalent to a larger circular radius than the considered radial extent. Therefore,  $C_{\text{mg}}$  is introduced in Equation (1) to account for this effect.

By default, galaxies in the primary sample are all central galaxies, while those in the secondary sample are satellites. We will consider the case of satellite-satellite pairs in section 3.2. If the satellite sample is statistically large enough, the influence of the circularity parameter would be averaged out. Therefore, the term related to the circularity parameter is not included here.

Considering  $v_c \approx \sqrt{\frac{G m_{1,v}}{r_{1,v}}}$  in the primary halo, where the virial mass  $m_{1,v}$  and virial radius  $r_{1,v}$  are defined in terms of 200 times the critical density of the universe, we

have

$$T_{\text{mg}} \propto \frac{m_{1,v}^{1/2} r_p^2}{G^{1/2} m_2 \ln \Lambda r_{1,v}^{1/2}}. \quad (2)$$

The Coulomb logarithm can be written as  $\ln \Lambda \approx \ln \frac{b_{\text{max}}}{b_{\text{min}}}$ , where  $b_{\text{max}}$  and  $b_{\text{min}}$  are the maximum and minimum impact parameters, respectively. When the satellite is initially outside the primary halo, and  $b_{\text{max}}$  approximates to the virial radius, we have  $\ln \Lambda \approx \ln \frac{m_{1,v}}{m_2}$ , if we take the virial velocity of the host halo as the initial velocity. In [Jiang et al. \(2008\)](#), they found that an alternative expression  $\ln(1 + \frac{m_{1,v}}{m_2})$  for the Coulomb logarithm performs better in explaining the time interval for the satellite between the time of entering the virial radius and merging with the central galaxy, mainly for the case of  $m_{1,v}/m_2 \leq 4$  where  $m_2$  is the virial mass of the satellite here. However, for galaxy pairs in smaller distance, where satellites are well within the virial radius, both  $b_{\text{max}}$  and  $b_{\text{min}}$  are very uncertain ([Hashimoto et al. 2003](#); [Peñarrubia et al. 2004](#); [Just et al. 2011](#)). We therefore do not explore the explicit influence of  $\ln \Lambda$ , while tentatively integrating both  $\ln \Lambda$  and  $C_{\text{mg}}$  into a constant coefficient in the following investigation.

Replacing  $T_{\text{mg}}$  in equation (1) with equation (2), we obtain

$$\Phi = A_* \frac{G^{1/2} m_2 r_{1,v}^{1/2} n_1 n_p(< r_p)}{m_{1,v}^{1/2} r_p^2}. \quad (3)$$

If Equation (3) holds, the coefficient  $A_*$  would be a constant, regardless of galaxy masses and redshift. We will verify this relation by checking on the reciprocal of  $A_*$ ,

$$\frac{1}{A_*} = \frac{1}{\Phi} \frac{G^{1/2} m_2 r_{1,v}^{1/2} n_1 n_p(< r_p)}{m_{1,v}^{1/2} r_p^2}. \quad (4)$$

which would also be a constant if the connection between merger rates and close pair counts can be established by Equation (3). Galaxy mergers are identified as in [Jiang et al. \(2008\)](#).

## 3. RESULTS

Equation (4) is obtained in the framework of dynamical friction, by assuming all merging pairs are central-satellite pairs. For satellite-satellite pairs that were central-satellite pairs before entering the primary halo, they may also merge. [Jiang et al. \(2010\)](#) showed that, this kind of merger is a similar process to that for central-satellite mergers. We will also examine if the relation formulated for central-satellite pairs applies to satellite-satellite pairs.

### 3.1. Central-Satellite Pairs

#### 3.1.1. Adopting Stellar Masses of Satellites

We know that one ruling factor of the dynamical process is the total mass of baryons and their surrounding dark matter in the satellite. As shown in [Jiang et al. \(2008\)](#), the total merging timescale between the time of entering the virial radius and the final coalescence can be established through the virial mass of the satellite. However, the total satellite mass varies at different stages of the merger. At the earlier stage when the satellite just enters the host halo, the dark matter mass dominates the satellite mass, and thus the merging timescale. While at

the later phase of the merging, the dark matter is mostly stripped off, and the stellar mass of the satellite determines when they finally coalesce. Therefore, at a middle stage when the two galaxies are  $\leq 100 h^{-1}\text{kpc}$  away, the satellite has partly lost its dark matter. The satellite mass  $m_2$  would be difficult to determine, making it the most uncertain quantity in Equation (4). As a first try, we use the stellar mass  $m_{2,s}$  to replace the satellite mass  $m_2$  in Equation (4).

We set the physical radial extent  $r_p$  to correspond to  $100 h^{-1}\text{kpc}$  in comoving space at all redshifts, as a trade-off between the statistics and the 'closeness'. In the left panel of Figure 1 we plot  $\frac{1}{A_*}$  obtained from Equation (4) as a function of satellite stellar mass  $m_{2,s}$  at a median redshift of  $z = 0.3$ . Four samples of central galaxies are shown by different colored lines, with stellar masses of 30.0 (black), 15.0 (red), 7.5 (green) and 4.0 (blue), respectively, in unit of  $10^{10} h^{-1}M_\odot$ . Galaxy pairs are selected down to a stellar mass ratio of 1 : 32, except for the lowest  $m_{1,s}$  for which the lowest  $M_{2,s}$  is not included, as galaxies at this mass consist of only  $\sim 30$  particles, and are subject to resolution effect. Error bars are plotted assuming poisson fluctuations for merger pairs. There is a tendency for  $\frac{1}{A_*}$  to decrease as the central stellar mass decreases. This can be attributed to the fact that, the satellite still has a significant fraction of dark matter within the comoving  $100 h^{-1}\text{kpc}$  from the host halo center. It is well indicated in the right panel of Figure 1, which displays the accumulated distribution of retained mass fraction of subhalos at  $z = 0.3$  since being accreted. The stellar mass ratio of the satellite inhabiting the subhalo to the central galaxy is above 1 : 30. Here subhalos are found and traced using a subhalo finder developed by Han et al. (2012), where the details of simulations can also be found. The virial masses of primary halos are similar to those hosting the central galaxies which are denoted with the same color in the left panel. Solid lines show results for subhalos around  $77 h^{-1}\text{kpc}$  (comoving  $100 h^{-1}\text{kpc}$  at  $z = 0.3$ ) away from the halo center. We can see that above 70% of subhalos still retain over 20% of their original mass before accretion. The retained mass is far more than the galaxy stellar mass residing in the center of the subhalo, given that the ratio of stellar mass to halo mass is at most a few percent (see, e.g., Behroozi et al. 2012). Even at a distance of  $10 - 60 h^{-1}\text{kpc}$  which is widely used in literature, above 40% of subhalos have a retained fraction of  $\geq 20\%$ . The total mass that is at work driving the merging outweighs the stellar mass of the galaxy. Therefore, it is not appropriate to only use the stellar mass when theoretically investigating the merger timescale problem.

Here we only assign the stellar mass to  $m_2$ , which would result in a different normalization in Equation (4) for different  $m_1$  (lines with different color in each panel of Figure 1). At the same stellar mass  $m_{2,s}$  for satellites, the total mass would be different. As the same  $r_p$  corresponds to a smaller fraction of the halo extent at larger host halos, satellites in larger host halos have gone deeper in the potential well and have lost a larger fraction of dark matter, as indicated in the right panel of Figure 1. Thus using the stellar mass instead of the total mass would bias  $m_2$  higher for more massive host halos.

On the other hand, modeled stellar components may not have the true masses compared to those in the real universe. As we know, the baryonic physics governing galaxy formation and evolution is not well understood yet, making it not easy for galaxies produced in hydro simulations to reconcile with those obtained in observations. This is also the case for semi-analytical models. Furthermore, there is no explicit correspondence between modeled galaxies and observed ones, particularly given the fact that it is very challenging for current hydro cosmological simulations to reproduce galaxies with sizes and shapes consistent with observed ones, induced by the uncertain physics implemented (Scannapieco et al. 2012). Thus we can not exactly tell what extent of a simulated galaxy corresponds to that observed for real galaxies. Therefore, theoretical merger timescales computed using the satellite stellar mass  $m_{2,s}$  would depend on both the baryonic physics implemented (how much stellar mass is produced) and the galaxy identification method (how much stellar mass is selected into a galaxy).

### 3.1.2. Accounting for Satellites' Mass Loss

As discussed above, the total mass of the satellite (stellar mass + retained dark matter mass) is what we need for  $m_2$  in Equation (4). However, it is not feasible to estimate the dark matter mass for observed satellites in a large statistical sample. In order to obtain a convenient way of relating galaxy pair counts to merger rates, as a second try we replace  $m_2$  with the virial mass of the satellite. Although the normalization would be different, it can be accounted for by a different constant  $B_*$ . One choice for the virial mass of the satellite is the infall mass which is the virial mass when the satellite was last a central galaxy. But it is hard to estimate the infall information from observations. We thus have a different try in which  $m_2$  is taken as the virial mass  $m_{2,v}$  that a central galaxy with the same stellar mass as the satellite would have at the redshift being considered. Given that the relation between the halo mass and stellar mass evolves slowly with time (see, e.g., Wang & Jing 2010; Behroozi et al. 2012; Yang et al. 2012), the two halo masses do not differ much. Now the virial masses both for the primary galaxy and for the satellite are set to be the value at the redshift being considered.

In the meantime, we need to model the mass loss of the satellite. Han et al. (2012) showed that the size of subhalos is proportional to the radius where the subhalo density equals the background density. Under the assumption of an isothermal sphere for the halo, we can easily deduce that the retained mass of the satellite is proportional to  $r_p$ . Therefore, we model the retained mass as  $m_{2,v} \frac{r_p}{r_{1,v}}$ .

On the other hand, the spherical collapse model of halos indicates  $v_c \propto H(z)r_{1,v}$ , where  $H(z)$  is the Hubble parameter at redshift  $z$ . Thus, we have  $m_{1,v} \propto r_{1,v}^3 \rho_{\text{crit}}(z) \propto \frac{v_c}{GH(z)}$ , in which  $\rho_{\text{crit}}(z)$  is the critical density at redshift  $z$ . We use this relation and  $v_c \approx \sqrt{\frac{Gm_{1,v}}{r_{1,v}}}$  to replace  $v_c$  and  $r_{1,v}$ , and account for the mass loss of subhalos in the dynamical friction formula. Then we obtain

$$T_{\text{mg}} \propto \frac{m_{1,v}}{m_{2,v}} [m_{1,v} GH_0 E(z)]^{-1/3} r_p, \quad (5)$$

where  $H_0$  is the Hubble parameter at  $z = 0$ , and  $E(z) = \Omega_v + \Omega_m(1+z)^3$ .

Equation (3) becomes

$$\Phi = B_* \frac{m_{2,v} n_1 n_p (< r_p) [m_{1,v} G H_0 E(z)]^{1/3}}{m_{1,v} r_p}. \quad (6)$$

Figure 2 shows that,  $\frac{1}{B_*}$  is nearly unchanged with respect to the primary galaxy mass and the satellite galaxy mass out to redshift 2. This means Equation (6) is valid to connect the number of close pairs to galaxy merger rate. We fit the  $\log \frac{1}{B_*}$  values for each primary galaxy to a straight line with zero slope. The four fitted values are then averaged to give a final result at each redshift. The resulting mean value of  $\log \frac{1}{B_*}$  is  $-0.23$  at  $z = 0.3$ ,  $-0.24$  at  $z = 0.8$ ,  $-0.25$  at  $z = 1.3$ , and  $-0.21$  at  $z = 2.0$ , respectively, shown as the dotted lines in the plot. These values are very close, giving a mean  $\frac{1}{B_*}$  of  $10^{-0.23}$  with fluctuations among different redshifts less than 10%. This indicates that the redshift dependence can be well accounted for by Equation (6).

Although the radial extent  $r_p$  varies at different redshifts in Figure 2, we explore the applicability of Equation (6) when other radial extent is adopted at the same redshift. Figure 3 shows results with  $r_p = 50/(1+z)h^{-1}\text{kpc}$  and  $150/(1+z)h^{-1}\text{kpc}$  at  $z = 0.3$ . In both cases,  $\frac{1}{B_*}$  is consistent with that obtained using  $r_p = 100/(1+z)h^{-1}\text{kpc}$  (dotted lines), which confirms the linear dependence of  $T_{\text{mg}}$  on  $r_p$ .

We make a check on the influence of the uncertain stellar mass. Jiang et al. (2010) found that even if the baryonic mass is halved in the simulation, the time needed for a satellite to merge with the central galaxy since entering the virial radius generally changes at the level of 10%. We therefore expect that the merger timescale for close galaxy pairs would change at a similar level if the stellar mass changes by less than 2 times. We show in Figure 4 the relation between the halo mass and stellar mass of the central galaxy for the lowest redshift case. Results are compared to those in Mandelbaum et al. (2006). It is clear that they are generally consistent, except for the highest mass bin where the halo mass is about 2.5 times smaller in our simulation. This can be attributed to the gas overcooling in massive halos, which results from the lack of AGN feedback to a certain degree. Since most massive galaxies are central galaxies, so that the overcooling mainly affects the identification of merger remnants, while taking little effect on the descending of satellites. Since the discrepancy between simulated galaxy masses and those in observations is far less than 2 times, we thus expect that baryonic physics implemented in our simulation can only induce an uncertainty of less than 10% in the relation shown in Figure 2.

Next we consider the influence of different galaxy identification method. Here we use a smaller linking length ( $b = 0.0125$ ) when identifying galaxies. Seen from Figure 5, the change is small when the new results are compared to the dotted lines which are the same as in Figure 2. The largest change happens at  $z = 2.0$ , where  $\frac{1}{B_*}$  is higher than that in Figure 2 by about 20%. Only the central core of a galaxy would be selected into a galaxy again after shortening the linking length. It makes

galaxies more easily stripped of particles, thus delaying the merger identification or reducing identified merger events. This explains why  $\frac{1}{B_*}$  is relatively higher here.

### 3.2. Satellite-Satellite Pairs

In section 3.1, we have obtained a good relationship between the merger rate and close number counts within  $100 h^{-1}\text{kpc}$  for central galaxies. We have considered the central-satellite pair which is the dominant merging pattern. However, the satellite-satellite merging pairs also exist, although they are minor in comparison to central-satellite pairs. We check in Figure 6 whether the scaling relation we have obtained still holds for satellite-satellite merging pairs. Dotted lines in each panel are the same as in Figure 2. At each redshift, most part of the four lines slightly lies above the dotted line. After applying the same fitting method as in Figure 2 to the data, the resulting amplitude is typically about 0.15 dex higher than those for central-satellite pairs in Figure 2. This higher amplitude results from the lower merger rate for satellite-satellite pairs, compared to that for central-satellite pairs with the same masses (Jiang et al. 2010). At small separation ( $\leq 100 h^{-1}\text{kpc}$ ), the contribution to pair counts from satellite-satellite pairs is at the level of 10% (see, e.g., Yoo et al. 2006). In view of the small increase in  $\frac{1}{B_*}$  for satellite-satellite pairs and the low fraction of such pairs, the influence of satellite-satellite pairs to the relation of merger rates and pair counts is expected to be very weak. We can therefore adopt the relation established only with central-satellite pairs.

### 3.3. Merger Timescales of Close Pairs

So far, all the investigations are done in the 3-dimensional frame. In observations, what we usually get is the projected number counts of galaxy pairs. To account for the projection effect, a correction factor  $f_{3d}$  is introduced to transfer projected pair counts  $N_p^{proj}$  to 3-dimensional counts,  $N_p = f_{3d} N_p^{proj}$ .

In Jiang et al. (2012), they found that the projected number density of satellites obeys a power-law form with the best-fit logarithmic slope of  $-1.05$ , and this profile is independent of both central galaxy luminosities and satellite luminosities. According to their Equation (8), for projected number of satellites within  $r_p^{proj}$  which is equivalent to number of pairs in the central-satellite case, it has a fraction  $f_{3d} = 66\%$  within the real 3-dimensional  $r_p$ . This fraction is the same for whatever the adopted  $r_p^{proj}$  is, given that the power-law slope is fixed for the radial distribution of galaxies. For satellite-satellite pairs, we use the simulation to check whether  $f_{3d} = 0.66$  is also applicable or not. We project all galaxies in the simulation box on the  $x - y$  plane while assuming the  $z$ -direction is along the line-of-sight, which is equivalent to selecting companions in a photometric survey with  $\frac{\Delta z}{1+z} \leq 0.015$ . We find that  $f_{3d} = 0.66$  are generally consistent with the simulation results, and thus can also be applied to satellite-satellite pairs.

According to  $T_{\text{mg}} = N_p(< r_p)/\Phi$ , where  $N_p(< r_p) = n_1 n_p(< r_p)$ , we can get from Equation (6) the merger timescale for galaxy pairs within  $r_p$ . Take into account the projection effect, for close pairs within a projected

distance of  $r_p^{\text{proj}}$ , the merger timescale

$$\frac{T_{\text{mg}}(< r_p^{\text{proj}})}{\text{Gyr}/h} = \frac{10^{-0.23}}{0.66} \frac{m_{1,v}}{m_{2,v}} [m_{1,v} G m_{1,v} H_0 E(z)]^{-1/3} \frac{r_p}{\text{kpc}/h} \quad (7)$$

Equation (7) offers us a method of computing the timescale for mergers between primary galaxies with stellar mass  $m_{1,s}$  and secondary galaxies with stellar mass  $m_{2,s}$  within a projected radius of  $r_p^{\text{proj}}$ . Besides the radial extent  $r_p^{\text{proj}}$  and redshift  $z$ , there are two other input quantities in Equation (7):  $m_{1,v}$  and  $m_{2,v}$ .  $m_{1,v}$  is the median virial mass of isolated halos which host a central galaxy of  $m_{1,s}$  at redshift  $z$ . Similarly,  $m_{2,v}$  is the median virial mass of isolated halos which host a central galaxy of  $m_{2,s}$  at redshift  $z$ . These virial masses, which are defined in terms of 200 times the critical density, can be estimated from the relation between dark halo mass and its central galaxy mass (e.g. Yang et al. 2003; Tinker et al. 2005; Mandelbaum et al. 2006; Wang et al. 2006; Yang et al. 2007; Zheng et al. 2007; Guo et al. 2010; Moster et al. 2010; Wang & Jing 2010; More et al. 2011; Li et al. 2012; Behroozi et al. 2012; Yang et al. 2012; Velander et al. 2013).

Next we make a comparison with results from Kitzbichler & White (2008) and Lotz et al. (2011). We calculate  $T_{\text{mg}}$  for galaxies more massive than  $4 \times 10^{10} h^{-1} M_\odot$  within a projected physical distance of  $100 h^{-1} \text{kpc}$  at  $z = 0.1$ . Kitzbichler & White (2008) gives a timescale of 9.0 Gyr for such mergers. Since their stellar mass ratio is between 1:1 and 1:4, we compute  $T_{\text{mg}}$  accordingly, finding  $T_{\text{mg}}$  is between 1.6 Gyr and 8.2 Gyr ( $h = 0.71$ ), corresponding to 1:1 mergers and 1:4 mergers respectively. The stellar mass is converted to halo mass using the relation between halo mass and its central stellar mass established in Mandelbaum et al. (2006). The timescale computed according to Kitzbichler & White (2008) (9.0 Gyr) is only close to that for 1:4 mergers in our results. On the other hand, the merger timescales for the same galaxies but within projected  $20 h^{-1} \text{kpc}$  are 0.31 Gyr (1:1) and 1.6 Gyr (1:4), by assuming  $T_{\text{mg}}$  is proportional to the outmost radius. These all indicate that a single timescale is not enough to describe mergers with stellar mass ratios in the range from 1:1 to 1:4. We need to consider the dependence of the timescale on both virial masses for the two galaxies.

#### 4. CONCLUSIONS

Using a high-resolution N-body/SPH cosmological simulation, we have studied the relation between galaxy pair counts and merger rates. Our results indicates that galaxy merger rates can be inferred from the number of close pairs as shown by Equation (6). Equivalently, the merger timescale can be established for galaxy pairs down to a stellar mass ratio of 1 : 30 out to redshift 2.0.

Studies based on stellar mass only may be subject to uncertainties in the theoretical modeling of baryonic physics and galaxy identification method in simulations. On the other hand, the dynamical friction time scale is determined by the dark matter surrounding galaxies. By using the virial mass of both galaxies in the close pair, we present an accurate scaling relation (Equation 7) for galaxy mergers within a projected distance  $r_p$ .

For major mergers (1:1-1:4) of galaxies above  $4 \times 10^{10} h^{-1} M_\odot$  at  $z = 0.1$ , estimated merger timescales ( $r_p < 100 h^{-1} \text{kpc}$ ) based on Equation (7) span a wide range from 1.6 Gyr to 8.2 Gyr ( $h = 0.71$ ), corresponding to 1:1 mergers and 1:4 mergers respectively. In contrast, the timescale given by Kitzbichler & White (2008) (9.0 Gyr) is only close to that for 1:4 mergers in our results. Our results indicate that a single timescale is not enough to describe mergers of stellar mass ratios even only from 1:1 to 1:4, and the dependence on the virial masses of the galaxies must be taken into account.

Although all the equations are formulated for central-satellite pairs, satellite-satellite merging can also be approximately described, with a typical deviation of 0.15 dex for the normalizing factor. This is a consequence of relatively lower merger rates for satellite-satellite pairs. Our results for the satellite-satellite can be incorporated into an accurate modeling the merger rate if the satellite fraction of galaxies is known (say, from HOD modeling (Zheng et al. 2007, e.g.)). Since the fraction of satellite-satellite pairs is low (at  $\sim 10\%$  level) the influence of such pairs to the relation of merger rates and pair counts is expected to be very weak. The relation established with central-satellite pairs can therefore be applied to all galaxies pairs to a good approximation.

This work is sponsored by NSFC (11121062, 10878001, 11033006, 11003035) and the CAS/SAFEA International Partnership Program for Creative Research Teams (KJCX2-YW-T23).

#### REFERENCES

- Behroozi, P. S., Wechsler, R. H., & Conroy, C. 2012, arXiv:1207.6105
- Bell, E. F., Phleps, S., Somerville, R. S., et al. 2006, ApJ, 652, 270
- Bezanson, R., van Dokkum, P. G., Tal, T., et al. 2009, ApJ, 697, 1290
- Binney, J., & Tremaine, S. 1987, Princeton, NJ, Princeton University Press, 1987, 747 p.,
- Boylan-Kolchin, M., Ma, C.-P., & Quataert, E. 2008, MNRAS, 383, 93
- Chou, R. C. Y., Bridge, C. R., & Abraham, R. G. 2011, AJ, 141, 87
- Cimatti, A., Nipoti, C., & Cassata, P. 2012, MNRAS, 422, L62
- De Lucia, G., & Helmi, A. 2008, MNRAS, 391, 14
- De Propriis, R., Conselice, C. J., Liske, J., et al. 2007, ApJ, 666, 212
- Guo, Q., White, S., Li, C., & Boylan-Kolchin, M. 2010, MNRAS, 404, 1111
- Han, J., Jing, Y. P., Wang, H., & Wang, W. 2012, MNRAS, 427, 2437
- Hashimoto, Y., Funato, Y., & Makino, J. 2003, ApJ, 582, 196
- Hilz, M., Naab, T., Ostriker, J. P., et al. 2012, MNRAS, 425, 3119
- Jiang, C. Y., Jing, Y. P., Faltenbacher, A., Lin, W. P., & Li, C. 2008, ApJ, 675, 1095
- Jiang, C. Y., Jing, Y. P., & Li, C. 2012, ApJ, 760, 16
- Jiang, C. Y., Jing, Y. P., & Lin, W. P. 2010, A&A, 510, A60
- Just, A., Khan, F. M., Berczik, P., Ernst, A., & Spurzem, R. 2011, MNRAS, 411, 653
- Kitzbichler, M. G., & White, S. D. M. 2008, MNRAS, 391, 1489
- Li, C., Jing, Y. P., Mao, S., et al. 2012, ApJ, 758, 50
- Le Fèvre, O., Abraham, R., Lilly, S. J., et al. 2000, MNRAS, 311, 565
- Lin, L., Koo, D. C., Willmer, C. N. A., et al. 2004, ApJ, 617, L9
- Lin, L., Patton, D. R., Koo, D. C., et al. 2008, ApJ, 681, 232
- Lotz, J. M., Jonsson, P., Cox, T. J., et al. 2011, ApJ, 742, 103

- Lotz, J. M., Jonsson, P., Cox, T. J., & Primack, J. R. 2010a, MNRAS, 404, 575
- Lotz, J. M., Jonsson, P., Cox, T. J., & Primack, J. R. 2010b, MNRAS, 404, 590
- Lotz, J. M., Jonsson, P., Cox, T. J., & Primack, J. R. 2008, MNRAS, 391, 1137
- Mandelbaum, R., Seljak, U., Kauffmann, G., Hirata, C. M., & Brinkmann, J. 2006, MNRAS, 368, 715
- McLure, R. J., Pearce, H. J., Dunlop, J. S., et al. 2013, MNRAS, 428, 1088
- More, S., van den Bosch, F. C., Cacciato, M., et al. 2011, MNRAS, 410, 210
- Moster, B. P., Somerville, R. S., Maulbetsch, C., et al. 2010, ApJ, 710, 903
- Naab, T., Johansson, P. H., & Ostriker, J. P. 2009, ApJ, 699, L178
- Newman, A. B., Ellis, R. S., Bundy, K., & Treu, T. 2012, ApJ, 746, 162
- Nipoti, C., Treu, T., Auger, M. W., & Bolton, A. S. 2009, ApJ, 706, L86
- Nipoti, C., Treu, T., Leauthaud, A., et al. 2012, MNRAS, 422, 1714
- Oogi, T., & Habe, A. 2013, MNRAS, 428, 641
- Patton, D. R., & Atfield, J. E. 2008, ApJ, 685, 235
- Patton, D. R., Carlberg, R. G., Marzke, R. O., et al. 2000, ApJ, 536, 153
- Patton, D. R., Pritchett, C. J., Carlberg, R. G., et al. 2002, ApJ, 565, 208
- Peñarrubia, J., Just, A., & Kroupa, P. 2004, MNRAS, 349, 747
- Scannapieco, C., Wadepuhl, M., Parry, O. H., et al. 2012, MNRAS, 423, 1726
- Springel, V. 2005, MNRAS, 364, 1105
- Tinker, J. L., Weinberg, D. H., Zheng, Z., & Zehavi, I. 2005, ApJ, 631, 41
- Velander, M., van Uitert, E., Hoekstra, H., et al. 2013, arXiv:1304.4265
- Wang, L., & Jing, Y. P. 2010, MNRAS, 402, 1796
- Wang, L., Li, C., Kauffmann, G., & De Lucia, G. 2006, MNRAS, 371, 537
- White, M. 2001, A&A, 367, 27
- Xu, C. K., Zhao, Y., Scoville, N., et al. 2012, ApJ, 747, 85
- Yang, X., Mo, H. J., & van den Bosch, F. C. 2003, MNRAS, 339, 1057
- Yang, X., Mo, H. J., van den Bosch, F. C., et al. 2007, ApJ, 671, 153
- Yang, X., Mo, H. J., van den Bosch, F. C., Zhang, Y., & Han, J. 2012, ApJ, 752, 41
- Yoo, J., Tinker, J. L., Weinberg, D. H., et al. 2006, ApJ, 652, 26
- Zheng, Z., Coil, A. L., & Zehavi, I. 2007, ApJ, 667, 760

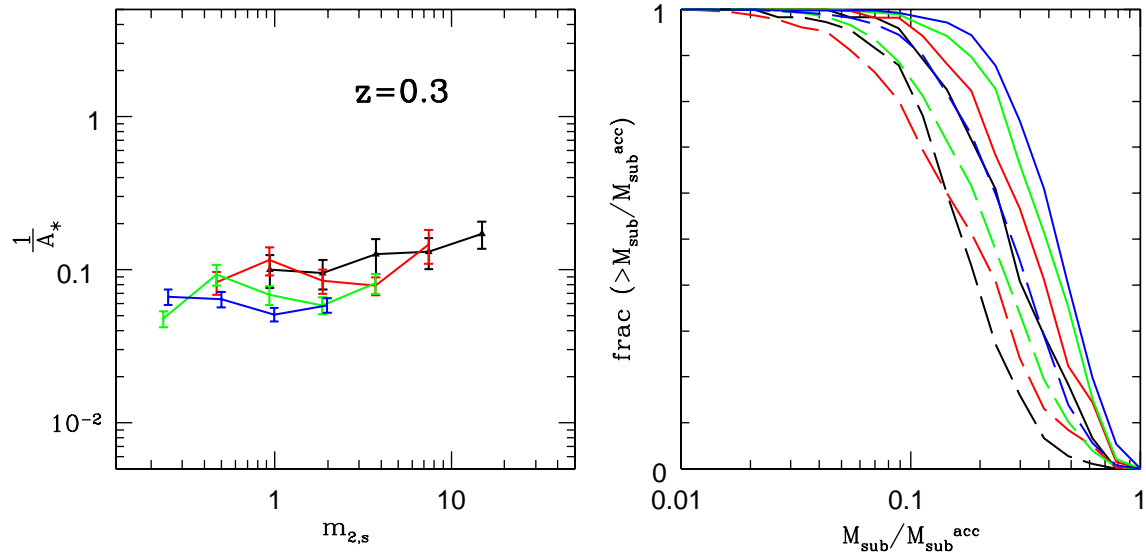


FIG. 1.— Left:  $\frac{1}{A_*}$  obtained according to Equation (4) when the stellar mass  $m_{2,s}$  is used for the satellite mass. Only central-satellite pairs are included. Four colored lines show samples with central stellar masses of 30.0 (black), 15.0 (red), 7.5 (green) and 4.0 (blue), respectively, in unit of  $10^{10} h^{-1} M_\odot$ . The outer radius corresponds to  $100 h^{-1} \text{kpc}$  in the comoving space. Right: Accumulated distributions of retained mass fraction of subhalos since accretion, for subhalos around  $77 h^{-1} \text{kpc}$  (comoving  $100 h^{-1} \text{kpc}$  at  $z = 0.3$ ) away from the halo center (solid lines), and those  $10 - 60 h^{-1} \text{kpc}$  away from the halo center at  $z = 0.3$  (dashed lines). The virial masses of primary halos are similar to those hosting the central galaxies which are denoted with the same color in the left panel. The stellar mass ratio of the satellite inhabiting the subhalo to the central galaxy is above 1 : 30.

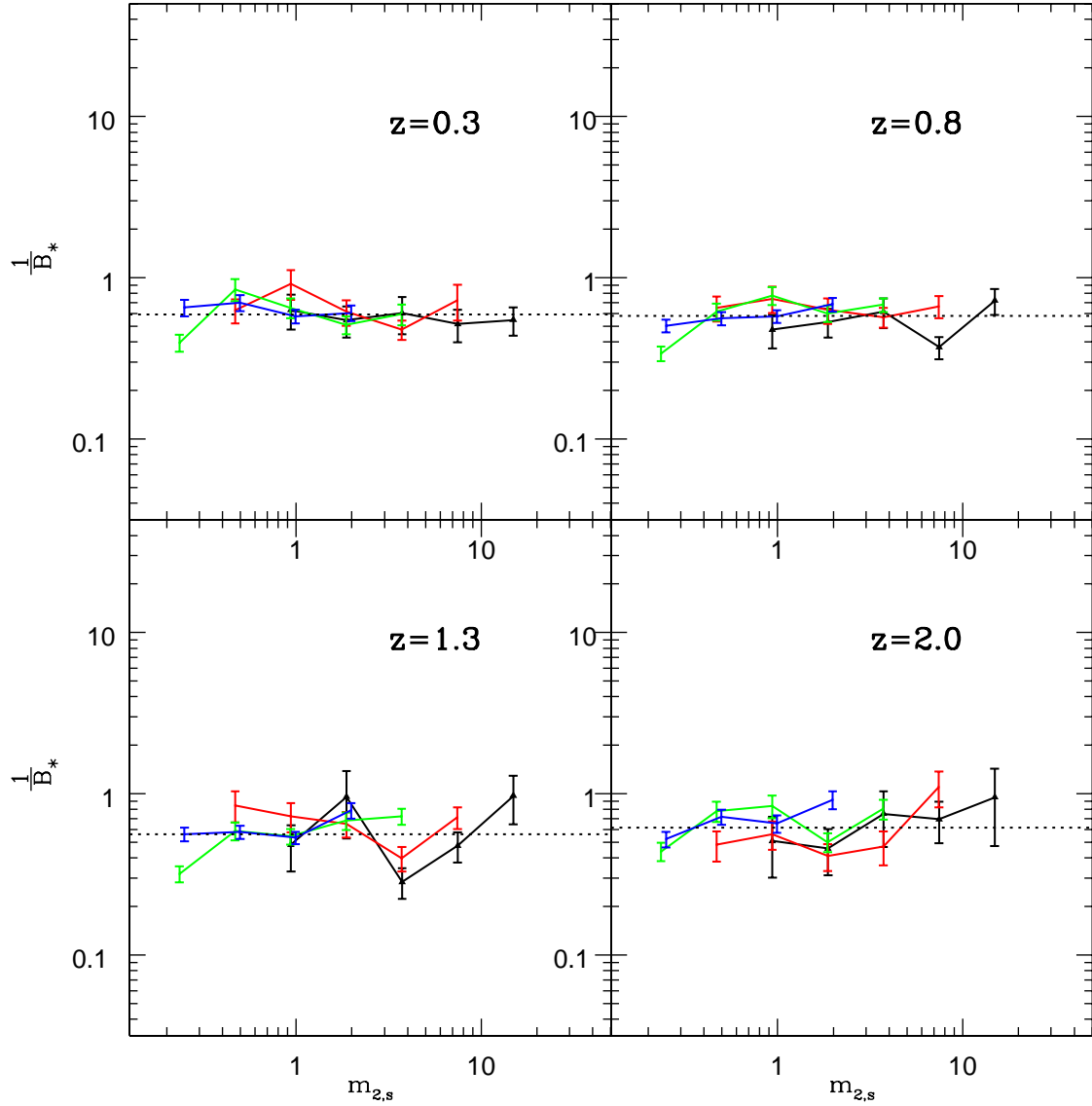


FIG. 2.— Same as the left panel of Figure 1, but the virial mass for satellites is used. Results are shown in 4 redshifts as displayed in different panels. The dotted lines are the fitting results at each redshift, showing  $\log_{10}(\frac{1}{B_*}) = -0.23, -0.24, -0.25, -0.21$  respectively, as the redshift increases.

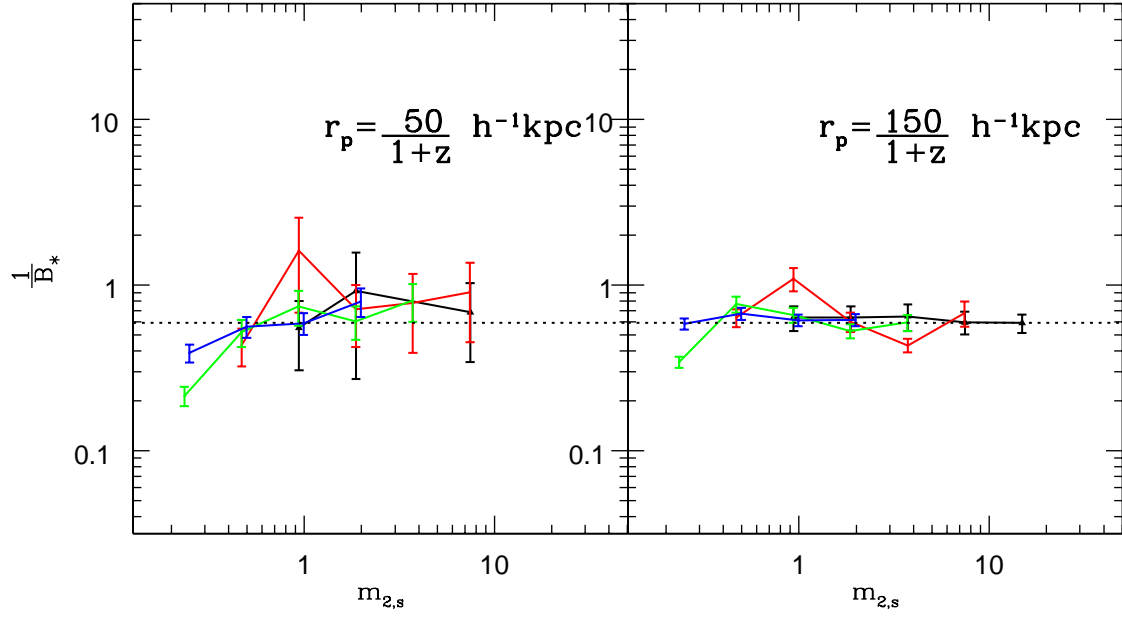


FIG. 3.— Same as the upper left panel in Figure 2, but the outer radius corresponds to  $50 h^{-1} \text{kpc}$  in the comoving space (left), and  $150 h^{-1} \text{kpc}$  in the comoving space (right).

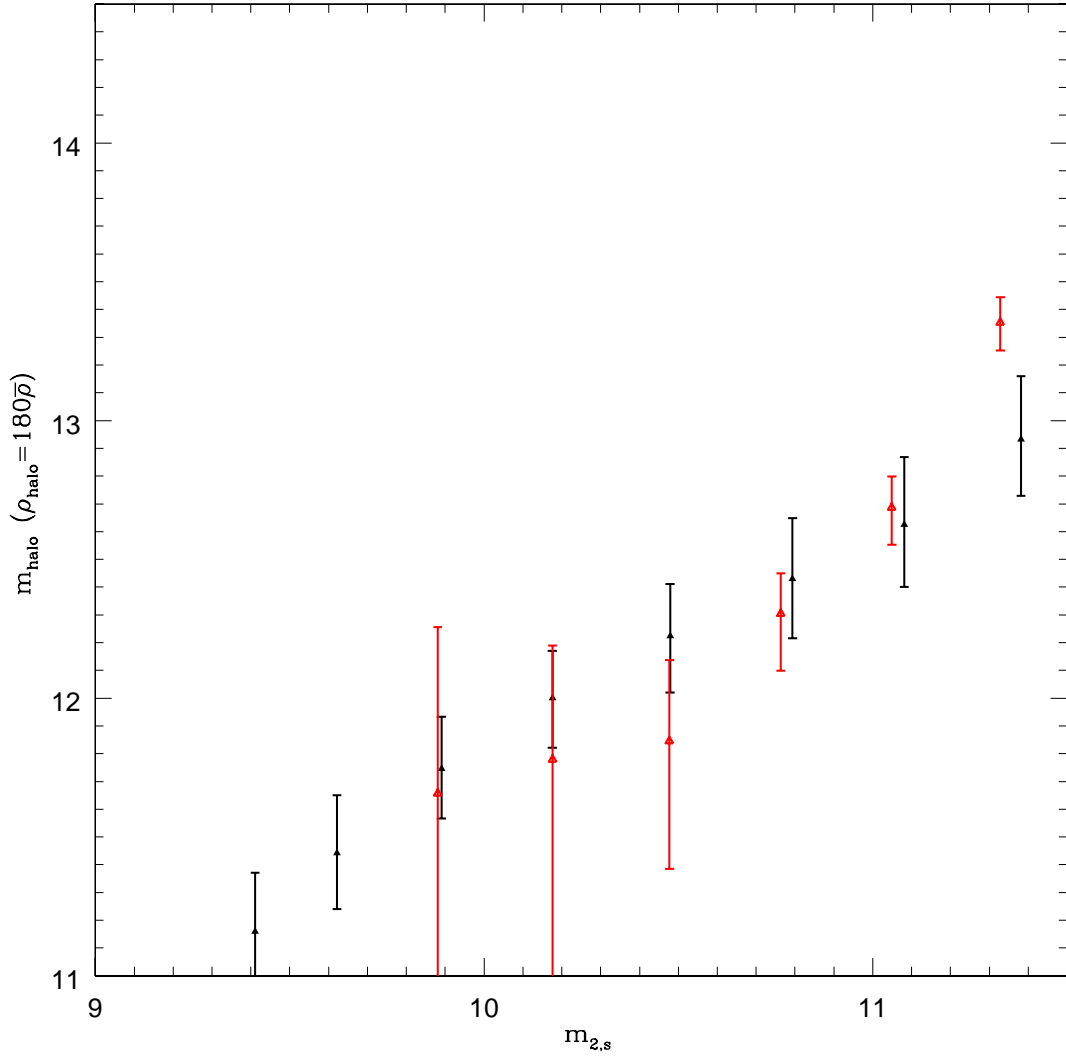


FIG. 4.— Median halo mass as a function of central stellar mass at  $z = 0.3$  (black points with error bars showing 68.3% interval). The bin width of the stellar mass is 0.3 in logarithmic space. To compare with the results from [Mandelbaum et al. \(2006\)](#) (red points), we define halo mass here as that enclosed within the radius, where the overdensity is equal to 180 times the mean density.

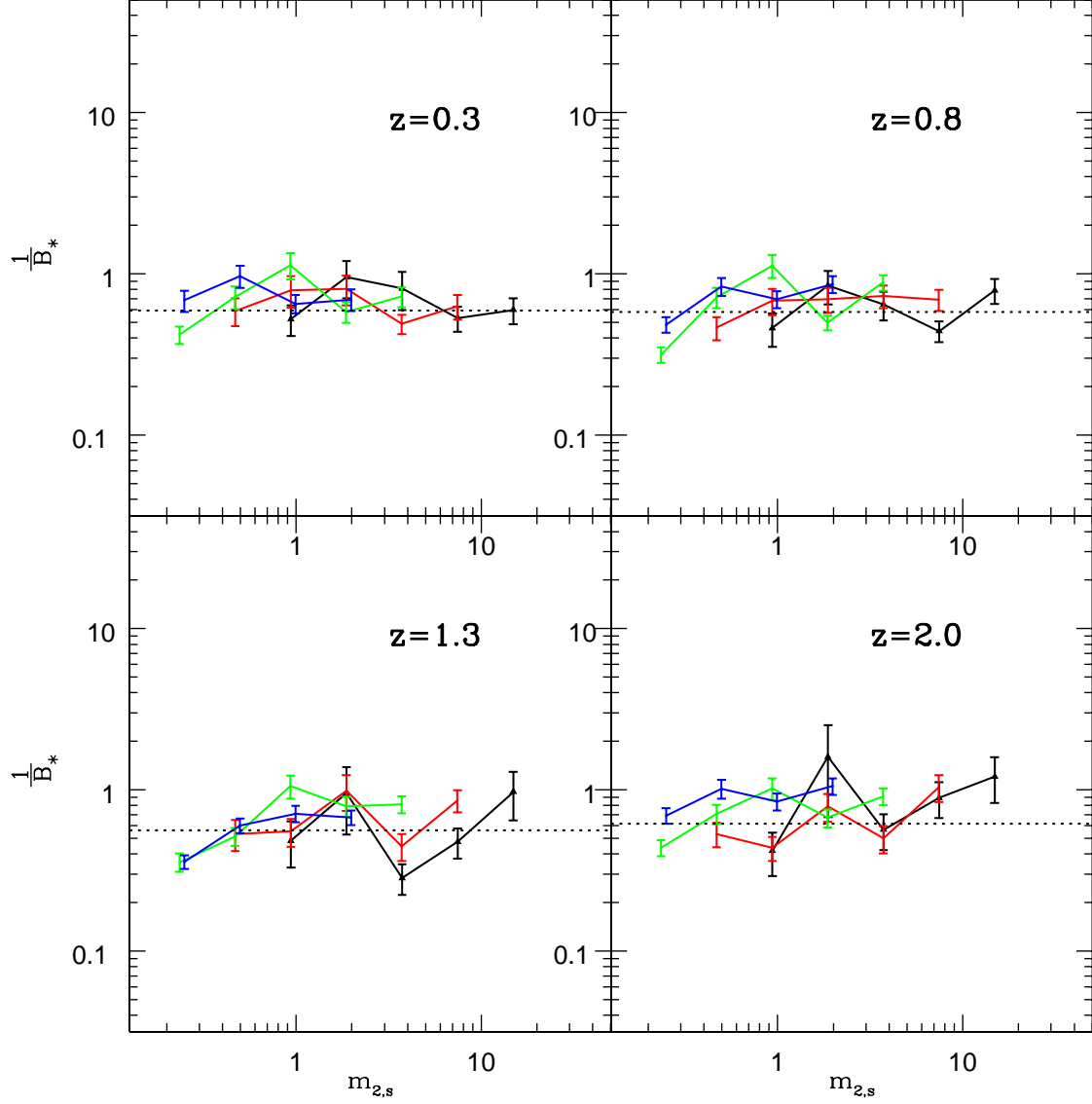


FIG. 5.— Same as Figure 2, but galaxies are linked with a smaller linking length ( $b = 0.0125$ ). Dotted lines are the same as those in Figure 2.

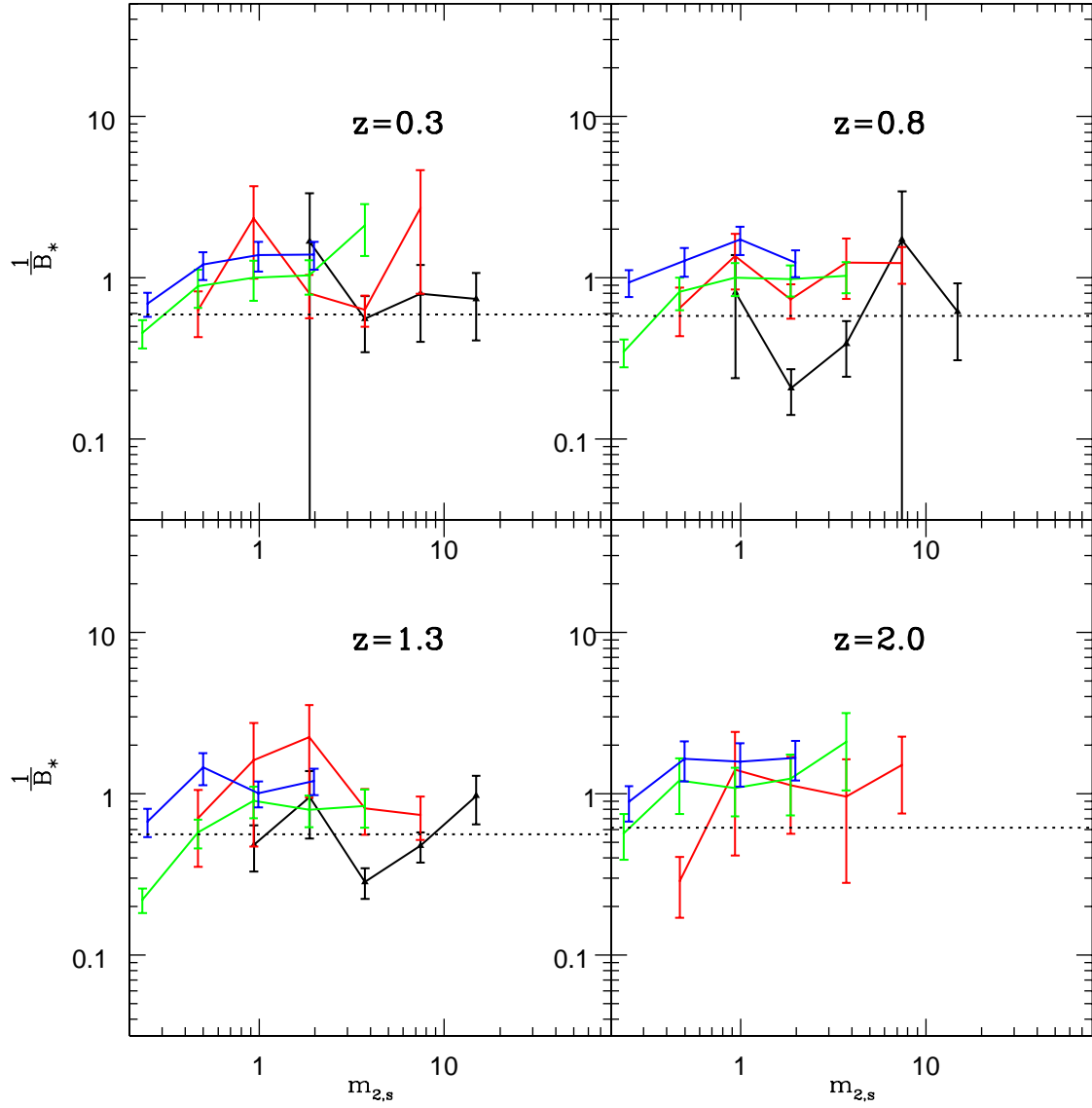


FIG. 6.— Same as Figure 2, but for satellite-satellite pairs. The dotted lines are the same as in Figure 2.